Characterization of the Plasma Plume from a LaB_6 Cathode: A Comparison of Probe Techniques

Robert L. Washeleski[1] and Lyon B. King[2]

Michigan Technological University, Houghton, MI, 49931, USA

Electrostatic probe diagnostics have been a staple of plasma research since the 1920s. Many probe theories and data-reduction techniques have been proposed and applied over the years to plasmas with a wide range of characteristics, which can lead to confusion when trying to determine which technique is appropriate for the application at hand. Four techniques were applied to a LaB_6 cathode plume in order to determine what the various techniques produced for a typical cathode plasma. A standard single-probe analysis was performed, as well as three different double-probe analyses using a hyperbolic tangent fit, a technique that looks at the peak separation in the second derivative, and a piece-wise linear fit. It was found that the cathode plasma was not entirely Maxwellian, and that the piece-wise linear fit stood out as being least susceptible to deviations from the ideal I-V characteristics. All four techniques yielded similar estimates of density, with the exception that the single-probe indicated noticeably lower densities within 10 mm of the cathode orifice. The single-probe also consistently indicated higher electron temperatures than the double-probes. The piece-wise double-probe technique indicated the lowest temperatures, with the other two double-probe techniques indicating temperatures approximately 50% higher.

Nomenclature

A_p	=	probe area (m^2)
e	=	elementary charge (C)
I_e	=	electron saturation current (A)
I_p	=	probe current (A)
i_N	=	ion saturation current N (A)
k	=	Boltzmann's constant (J/K)
m_e	=	electron mass (kg)
m_i	=	ion mass (kg)
n_e	=	electron number density (m^{-3})
T_e	=	electron temperature (Kelvin)
V	=	probe voltage (V)
V_p	=	plasma potential (V)
λ_D	=	Debye length (m)

I. Introduction

ELECTROSTATIC probes have been a fundamental plasma diagnostic technique since the work of Mott-Smith and Langmuir in the mid-1920s[1]. Commonly called Langmuir probes, this class of probe consists of a small metal electrode which is immersed in the plasma. Tungsten wire is typically used for ease of construction. The probe is biased over a range of voltages both positive and negative with respect to the plasma, with the collected current providing information about the plasma conditions[2]. Langmuir probes have the advantage of providing local measurements of plasma properties, but the disadvantage of complicated theory required to interpret the resulting I-V characteristic. While the theory of probes predicts characteristics that are simple to dissect, actual probe data

[1] Ph.D Candidate, ME-EM Dept., 815 R.L. Smith Bldg., 1400 Townsend Dr.
[2] Associate Professor, ME-EM Dept., 1018 R.L. Smith Bldg., 1400 Townsend Dr.

typically provides traces that deviate from theory. Because of this, many theories and probe data-reduction techniques have been proposed, based on a variety of different assumptions and probe techniques. The widespread use of Langmuir probes on a large array of plasmas and the equally large array of interpretation schemes used lends confusion as to which is appropriate for electric propulsion plasmas.

The subject of this paper is a comparison of four different probe techniques performed on a laboratory LaB_6 cathode typically used for electric propulsion experiments. One single-probe technique and three double-probe techniques were implemented and compared. Of secondary interest is the effect of background pressure on the plume of a cathode, provided by injecting argon gas into the vacuum chamber at variable flow rates. This work will be followed in later publications by implementation of a laser Thomson scattering diagnostic (LTS), with the probe data used a baseline with which to compare to direct measurements of electron temperature and density. Thomson scattering is a laser diagnostic technique where a pulse or series of pulses from a laser are sent into a plasma and the scattered spectra are recorded. Using this technique the electron energy distribution function, rather than just temperature, and plasma density can be determined in a non-invasive way from the intensity and shape of the measured spectra[3].

II. Experimental Apparatus and Methods

A. Vacuum Facility

Cathode characterization was performed in the Michigan Technological University (MTU) Ion Space Propulsion (ISP) Lab's Condensible Propellant Test Facility (CPTF). The CPTF is a 2-m-diameter by 4-m-long stainless steel cylindrical vacuum tank with a base pressure below 10^{-6} Torr. Rough vacuum is attained with a 400 cfm two-stage mechanical pump. High vacuum is provided by three Leybold Mag-2000 turbomolecular pumps with a combined pumping speed of 6000 l/s.

B. Cathode and Anode

The cathode used was a laboratory cathode with a LaB_6 emitter fabricated in the ISP Lab. The body is made of titanium and measures approximately 25 mm in diameter by 100 mm long. The cathode orifice is 4 mm in diameter. All tests reported here utilized krypton as a discharge gas. A tungsten keeper electrode is placed approximately 3.5 mm from the cathode face. A schematic of the cathode can be seen in Figure 1.

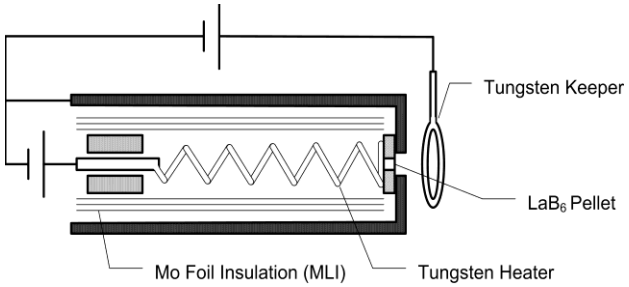

Figure 1. LaB_6 laboratory cathode.

The anode was a flat, circular stainless steel plate 125 mm in diameter placed approximately 125 mm downstream of the cathode keeper. The cathode discharge was started with the keeper, and then all current was attached to the anode through a Sorenson DHP power supply in current-limited mode. The discharge current was fixed at 7 amps and the propellant mass flow was fixed at 12 sccm. Argon gas was injected at a controlled flow rate into the vacuum chamber in order to elevate the background pressure. The cathode was operated at tank pressures of 4.5×10^{-5} Torr, 6.1×10^{-5} Torr, 8.3×10^{-5} Torr, and 1.0×10^{-4} Torr. Anode to cathode voltage at these pressures was 50 V, 48 V, 45 V, and 43 V, respectively. A schematic of the anode and cathode can be seen in Figure 2.

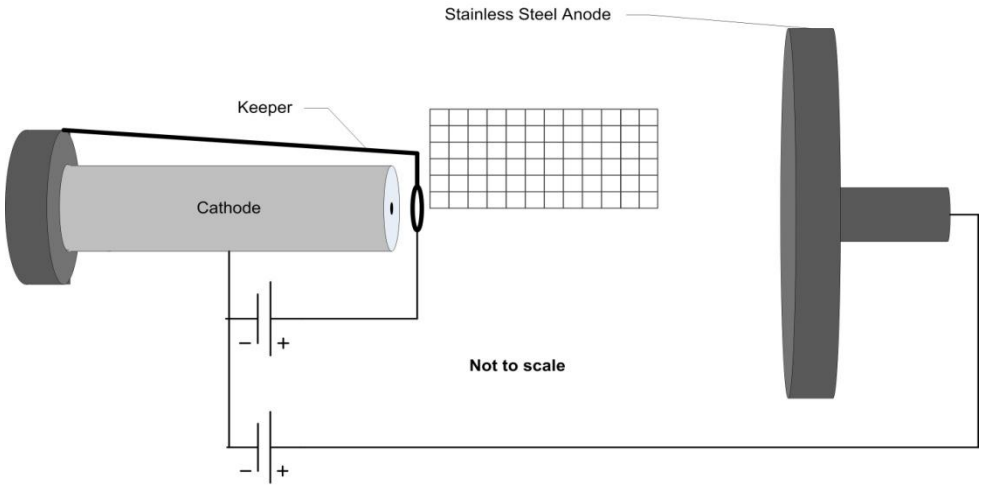

Figure 2. Electrical schematic showing cathode, anode, and measurement grid locations (top view).

C. Probes

The electrostatic probes used consist of two tungsten wires 0.05" in diameter inside an alumina sheath. The protruding length of the wires is 3.8 mm. The probes were mounted on a 3-axis motion table, which allows mapping of the cathode plume for comparison with future LTS measurements. The probes were driven with a programmable source meter controlled by an automated measurement program written in G. The probes were swept from -50 to 50 V in 0.1 V steps, with a measurement time of 16 msec at each voltage. Five sweeps were recorded at each measurement location for both single and double probe traces, with the actual voltage and collected current recorded. Measurement locations formed a rectangular grid 30 mm by 60 mm with 5 mm spacing covering half of the plume, which was assumed to be roughly symmetric based on past probe studies. Sweeps were performed in pseudo-random order, with a complete data set taking between 60 and 90 minutes to complete.

D. Single Probe Analysis

In order to handle the large number of traces, an automated analysis program was written in Python. The general algorithm is similar to the process suggested by David Pace[4]:

1) Average and smooth the 5 traces taken at each grid point
2) Fit the ion saturation region with a line
3) Find floating potential
4) Subtract the ion saturation current in order to get rid of negative values
5) Take the natural log of the current
6) Fit the electron saturation region with a line
7) Fit the exponential electron region with a line
8) Find the plasma potential (intersection of the lines in steps 6 and 7)
9) Calculate T_e from the slope of step 7
10) Calculate electron density

Floating potential was taken to be the zero crossing of the line fit to the ion saturation region. The electron saturation region usually was clearly linear after the natural log of the current was taken, but the exponential electron current region was less linear, as can be seen in Figure 3.

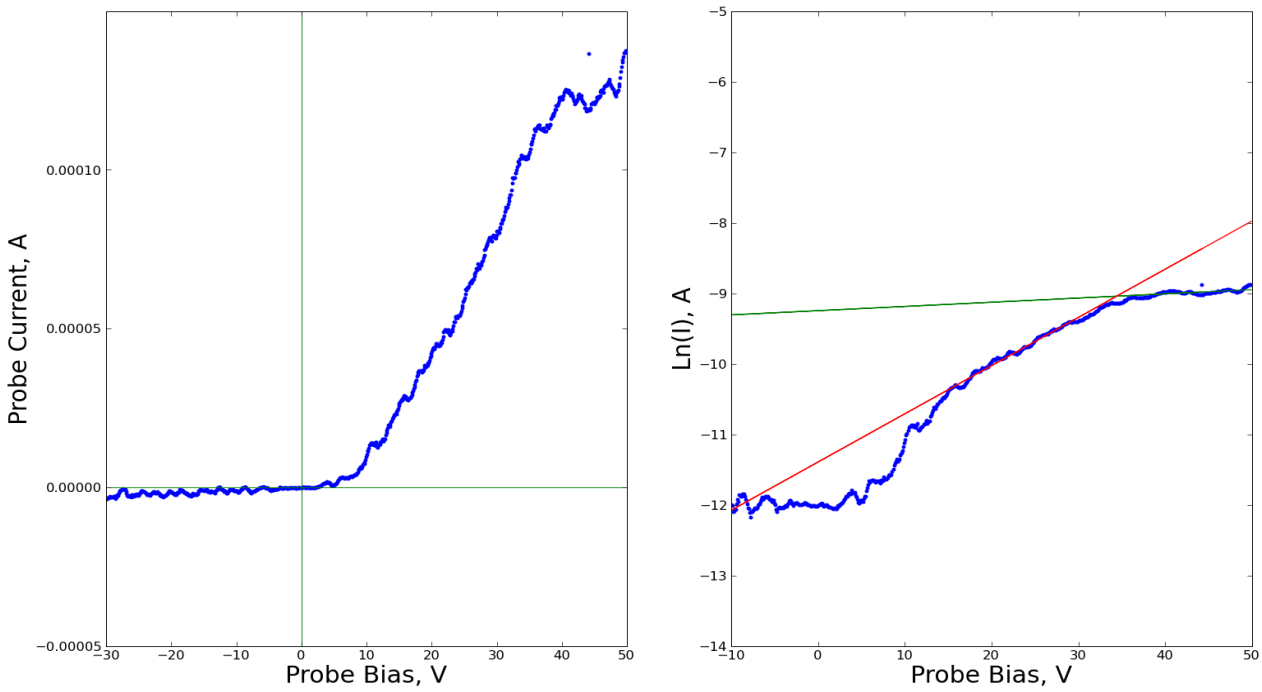

Figure 3. Left: Smoothed single probe trace. Right: Fit of exponential electron current region and electron saturation region, where the intersection is taken to be plasma potential.

The inverse of the slope of the red line in Figure 3 (from step 7) is equal to the electron temperature in eV. This value was then used to calculate the electron density according to:

$$n_e = \frac{I_{sat}}{eA_p}\sqrt{\frac{m_i}{kT_e}} \qquad \text{(Eq. 1)}$$

E. Double Probe Analysis

Double probe trace evaluation was also automated using a Python program. There are several ways to analyze double probe traces, and three were compared in this work. The first two methods apply to the special case when both probe tips are of the same area, which leads to a hyperbolic tangent I-V characteristic. For these experiments the probes were as close in size as we could make them. The probe data were smoothed and a least-squares hyperbolic tangent fit was performed according to the following equation:

$$I_p(V) = A \cdot \tanh[B \cdot (V - E)] + C \cdot x + D \qquad \text{(Eq. 2)}$$

where *A* is the ion saturation current and *B* is proportional to the inverse of the electron temperature. The other coefficients are required to perform the fit, but are not of physical significance. This technique will be referred to as the hyperbolic tangent technique.

The second method that was implemented was found in the work of Amemiya[5]. This method uses the second derivative of the probe data to estimate the electron temperature. Differentiating the raw data was not possible due to noise, and even the smoothed data had too much noise for direct differentiation. Instead, a hyperbolic tangent fit to the smoothed data was found and the resulting function was differentiated twice, yielding a somewhat idealized curve. The separation between peaks was determined, and used to compute the electron temperature according to:

$$T_e = \frac{\Delta V}{2\ln(2+\sqrt{3})k} \qquad \text{(Eq. 3)}$$

This new electron temperature was then used to solve for electron density using Eq. 1.

The third method of double probe analysis that was used is that of Chen[2]. Three piece-wise linear fits are performed, one near zero volts and two on the ion saturation current portions of the curve. The intersection of the saturation fits with the y-axis are taken to be the saturation currents, and the slope at the origin is proportional to the inverse of the electron temperature, given by the following:

$$\left.\frac{dI}{dV}\right]_0 = \frac{e}{kT_e}\frac{i_1 \cdot i_2}{i_1 + i_2} \qquad \text{(Eq. 4)}$$

The electron density is then calculated using Eq. 1. For a probe with tips of equal area the saturation currents will be equal, but this method does not require that to be the case.

III. Results

A. Electron Density

For all background pressures the electron density was found to be between 3 x 10^{15} m^{-3} and 2 x 10^{17} m^{-3}. Electron density near the orifice increased as background pressure was increased. The mass flow rate was held constant at 12 sccm Kr, and discharge current was held at 7 amps. The results can be seen in Figures 4-7.

Single Probe

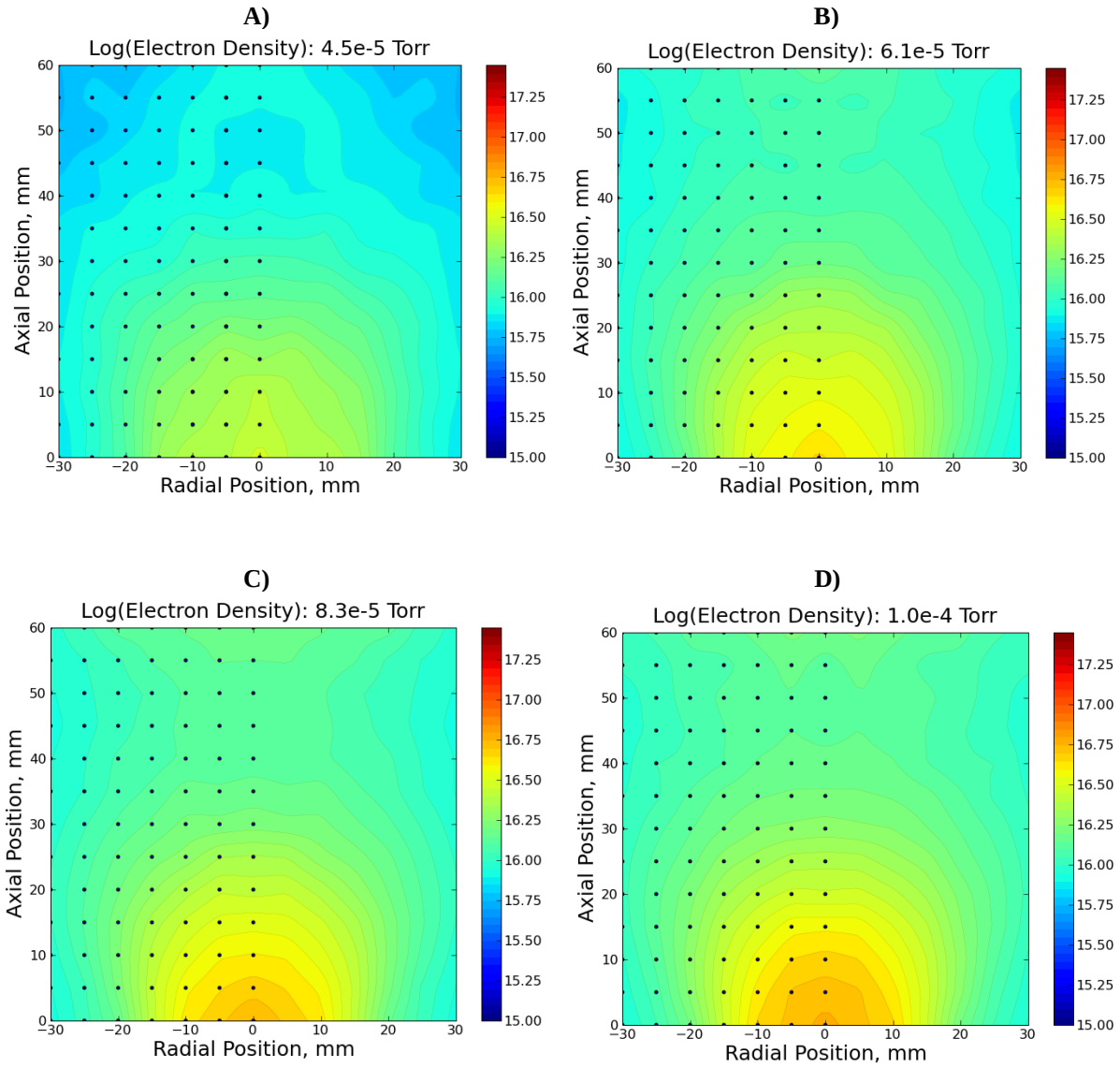

Figure 4. Logarithm of electron number density as measured by the single probe at A) 4.5 x 10^{-5} Torr, B) 6.1x 10^{-5} Torr, C) 8.3 x 10^{-5} Torr, and D) 1.0 x 10^{-4} Torr.

Double Probe (Hyperbolic Tangent)

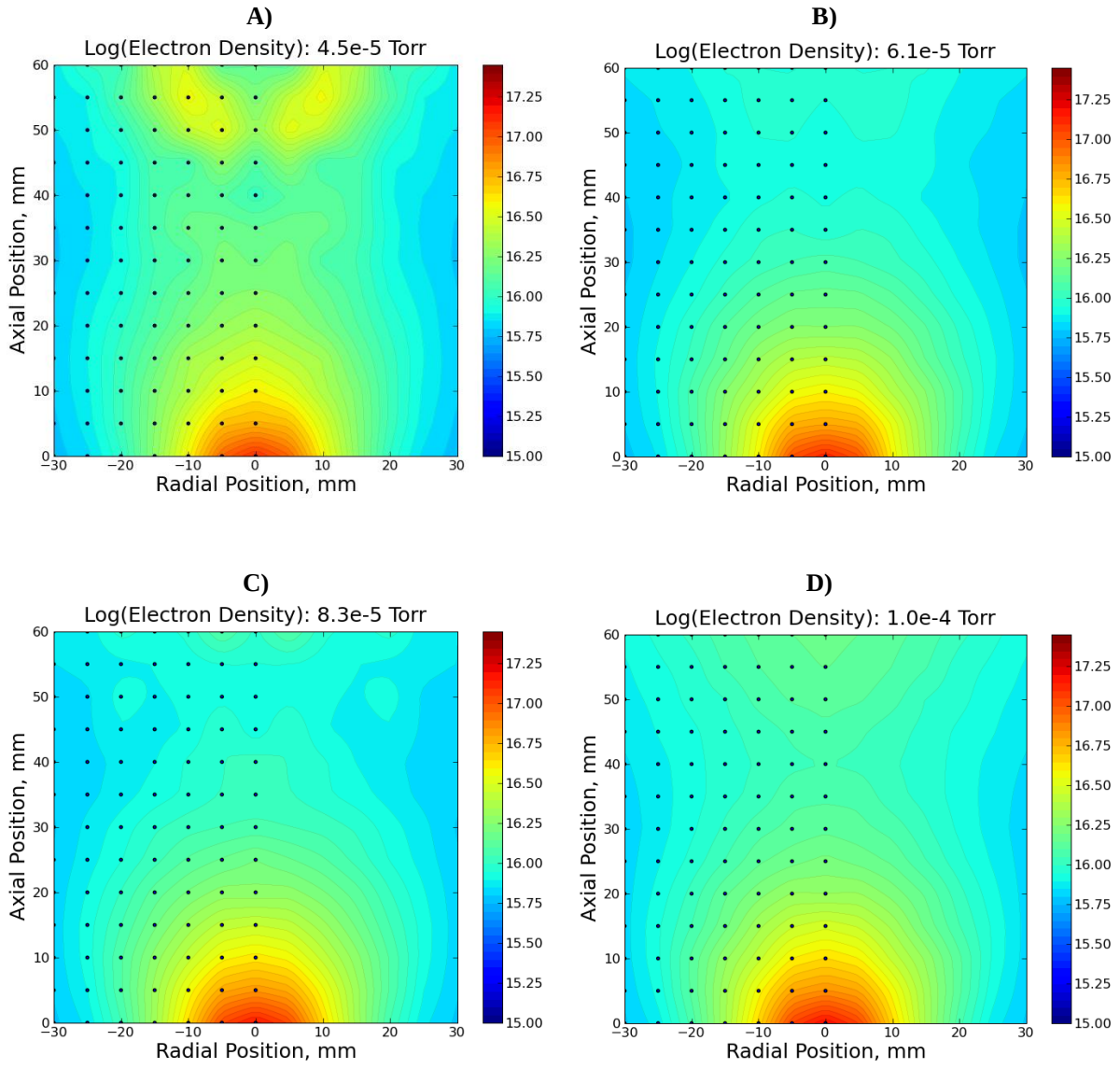

Figure 5. Logarithm of electron number density as measured by hyperbolic tangent fit at A) 4.5 x 10^{-5} Torr, B) 6.1x 10^{-5} Torr, C) 8.3 x 10^{-5} Torr, and D) 1.0 x 10^{-4} Torr.

Double Probe (Amemiya)

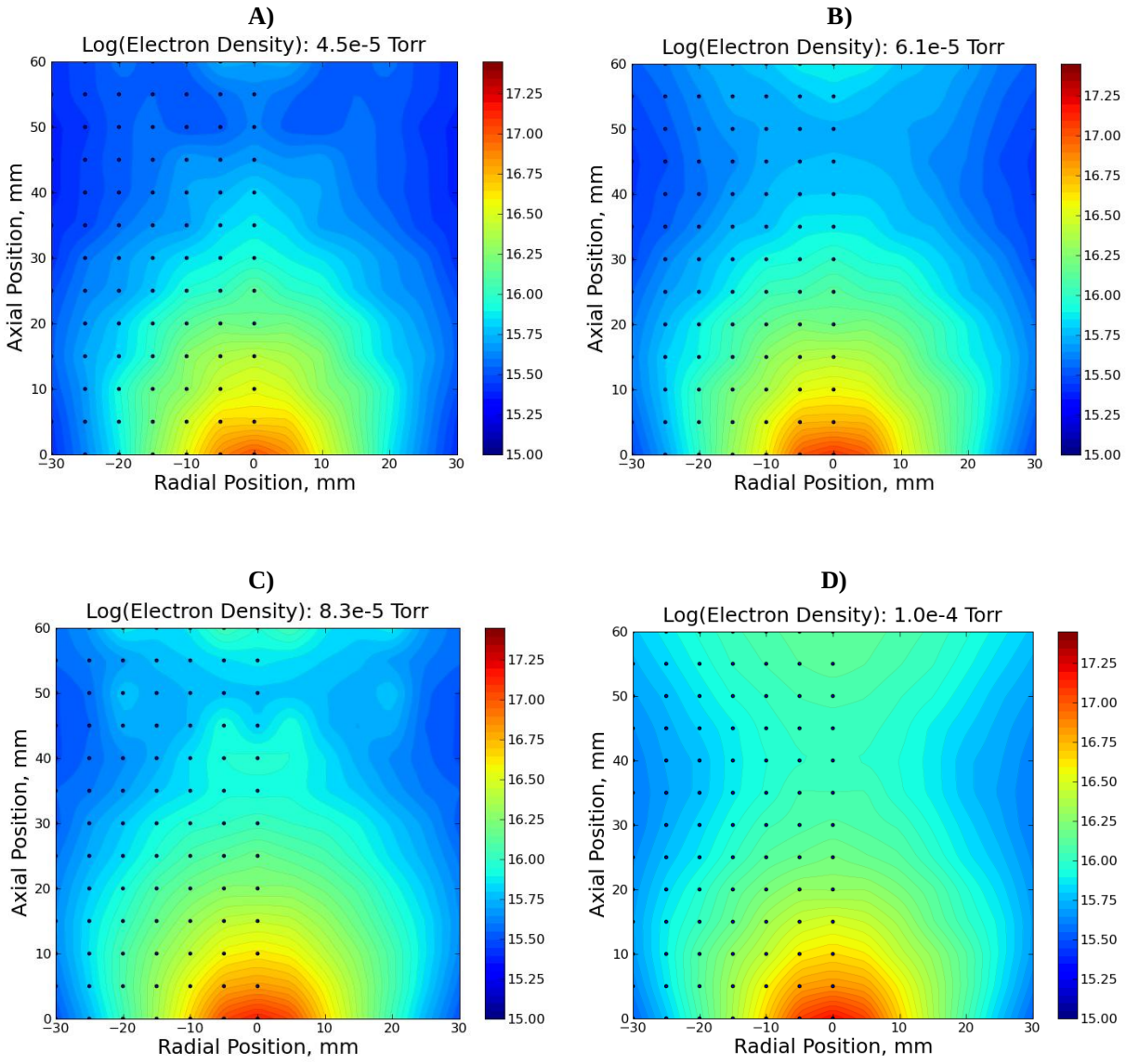

Figure 6. Logarithm of electron number density as measured by Amemiya's method at A) 4.5 x 10^{-5} Torr, B) 6.1x 10^{-5} Torr, C) 8.3 x 10^{-5} Torr, and D) 1.0 x 10^{-4} Torr.

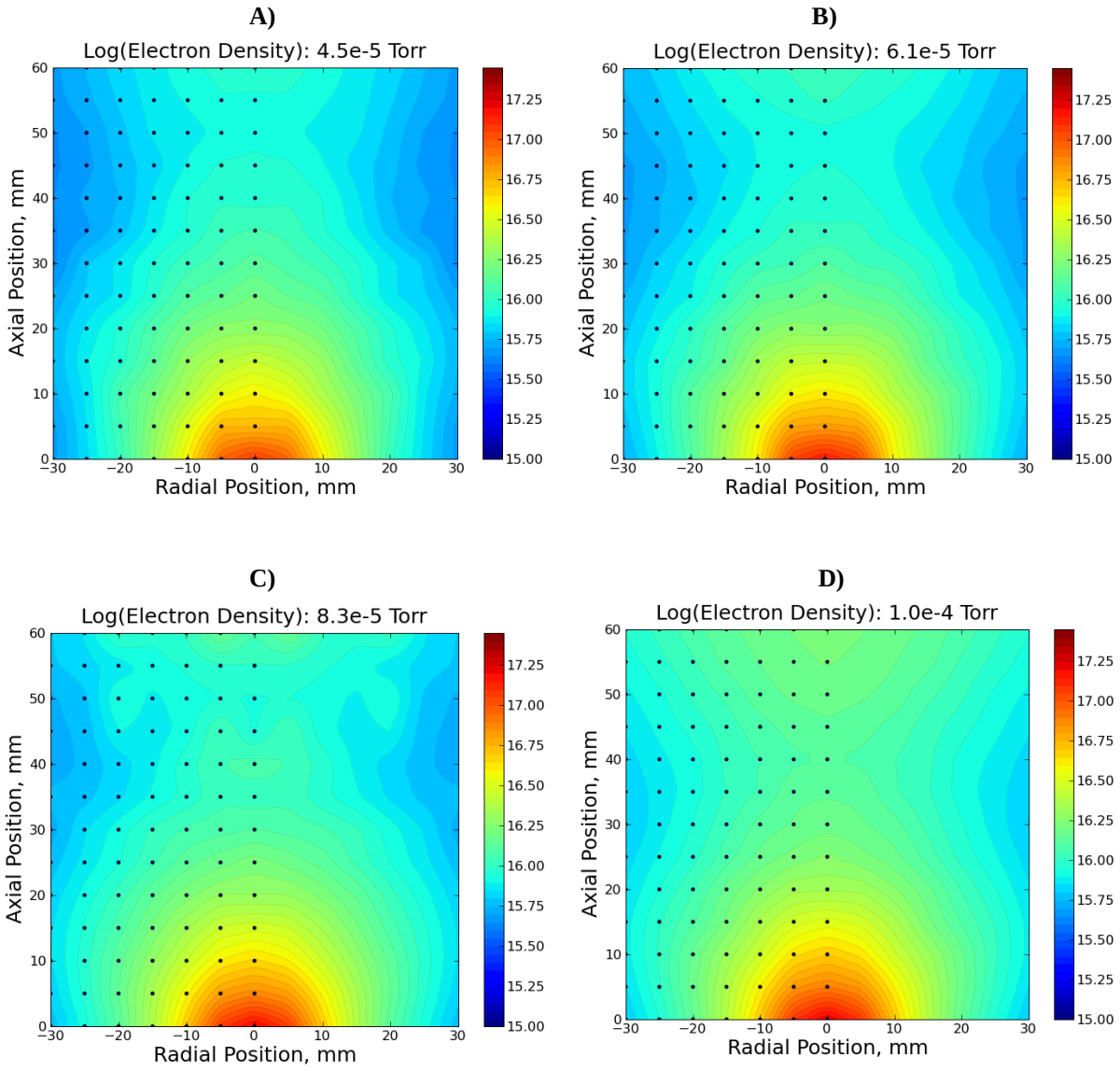

Figure 7. Logarithm of electron number density as measured by Chen's method at A) 4.5 x 10^{-5} Torr, B) 6.1x 10^{-5} Torr, C) 8.3 x 10^{-5} Torr, and D) 1.0 x 10^{-4} Torr.

B. Electron Temperature

The electron temperatures exhibited significant variation across different probe techniques, especially at locations more than 3 cm away from the cathode orifice. Areas that are white indicate probe traces that could not be properly fit due to deviation from the model used. Differences will be discussed in the next section. The results can be seen in Figures 8-11.

Single Probe

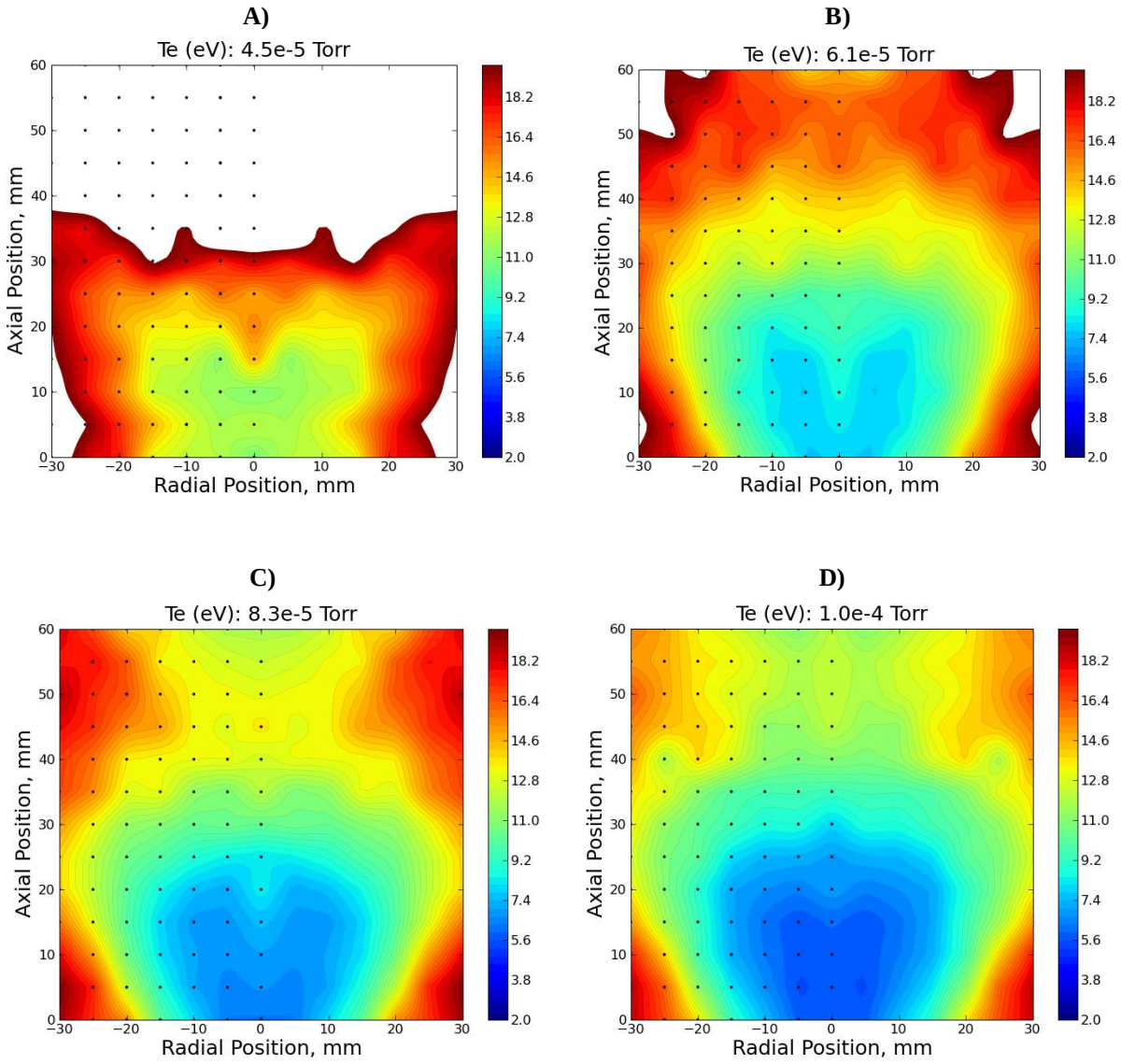

Figure 8. Electron temperature as measured by the single probe at A) 4.5 x 10^{-5} Torr, B) 6.1x 10^{-5} Torr, C) 8.3 x 10^{-5} Torr, and D) 1.0 x 10^{-4} Torr.

Double Probe (Hyperbolic Tangent)

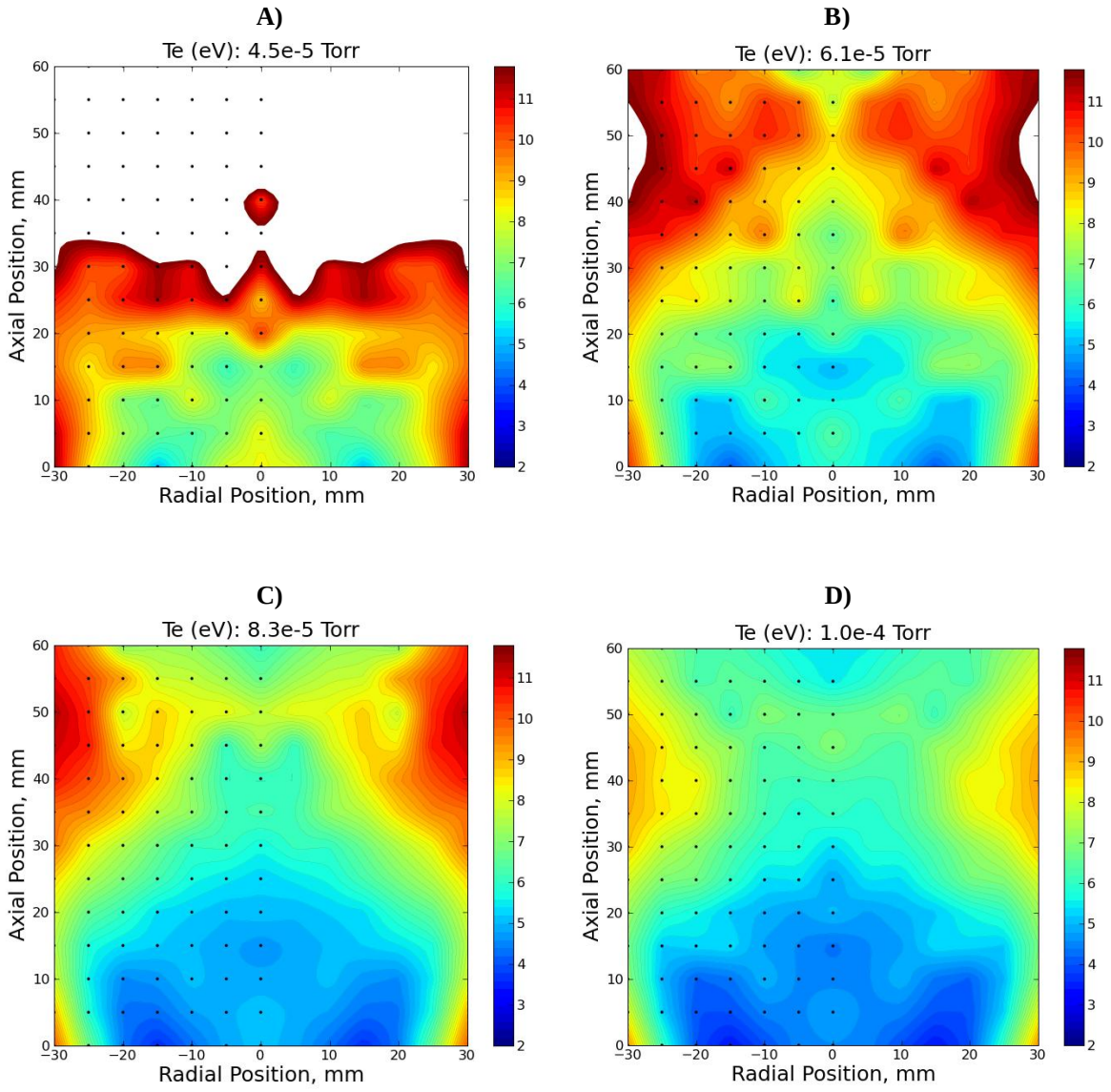

Figure 9. Electron temperature as measured by hyperbolic tangent fit at A) 4.5 x 10^{-5} Torr, B) 6.1x 10^{-5} Torr, C) 8.3 x 10^{-5} Torr, and D) 1.0 x 10^{-4} Torr.

Double Probe (Amemiya)

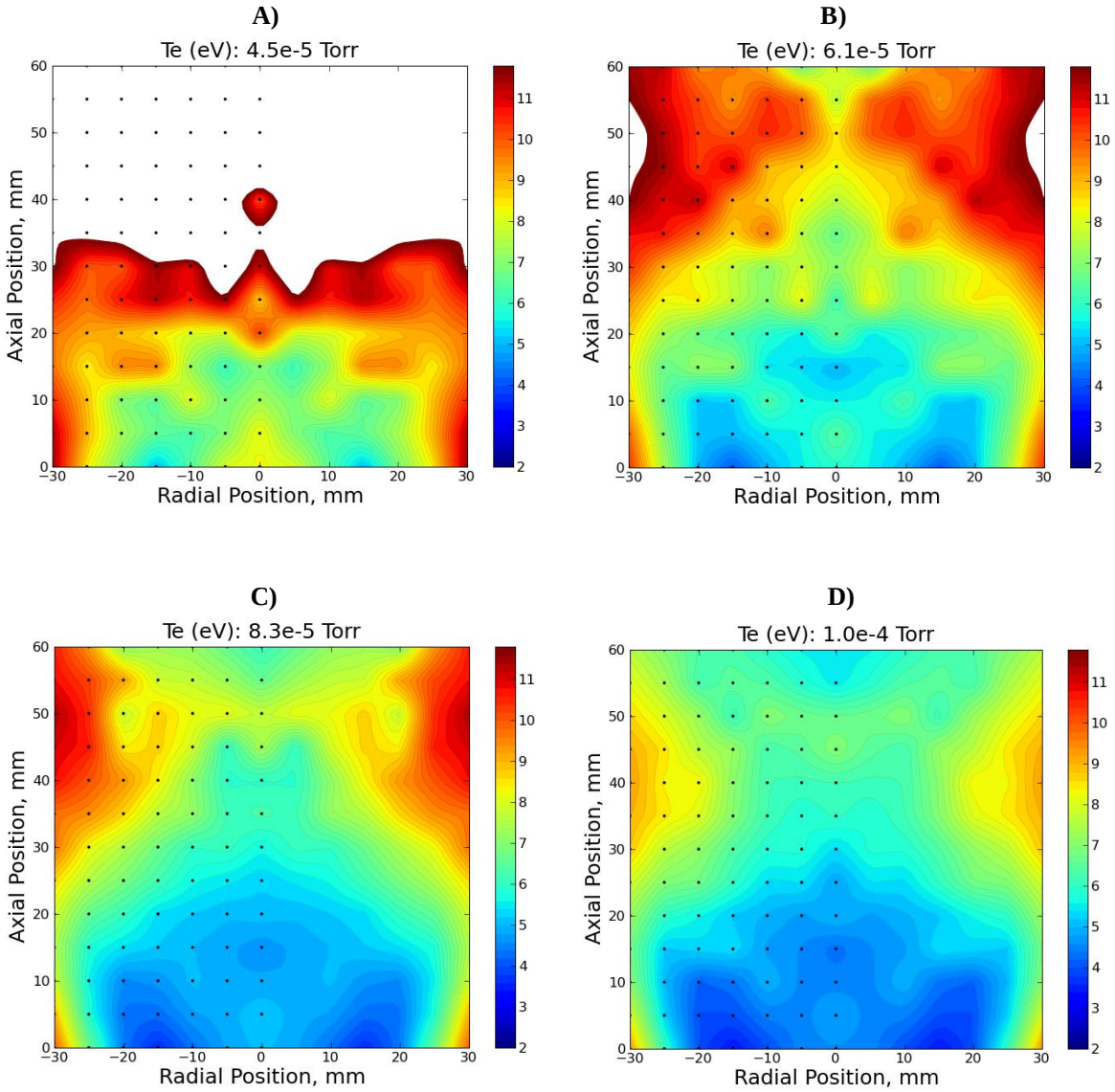

Figure 10. Electron temperature as measured by Amemiya's method at A) 4.5 x 10^{-5} Torr, B) 6.1x 10^{-5} Torr, C) 8.3 x 10^{-5} Torr, and D) 1.0 x 10^{-4} Torr.

Double Probe (Chen)

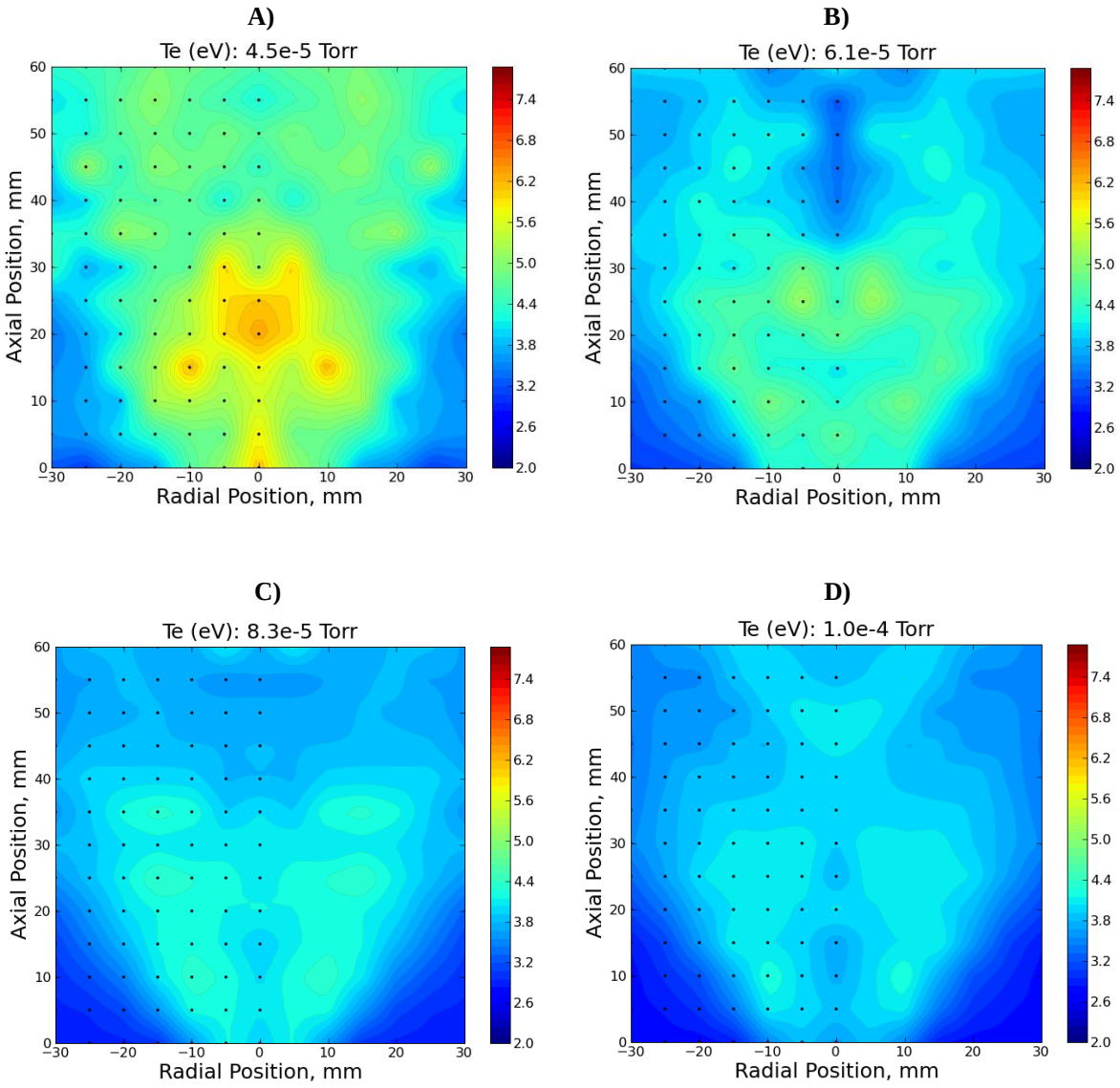

Figure 11. Electron temperature as measured by Chen's method at A) 4.5 x 10^{-5} Torr, B) 6.1x 10^{-5} Torr, C) 8.3 x 10^{-5} Torr, and D) 1.0 x 10^{-4} Torr.

C. Plasma Potential

All plasma potentials are relative to the cathode body. Plasma potential was calculated using the technique described in section II. D. for the single probe. For the double probe, the voltage of one probe with respect to the cathode body was recorded with each sweep. The voltage that is recorded when the applied voltage between the probes is zero is the floating potential. Using the floating potential and the electron temperature the plasma potential was calculated from the following equation:

$$V_p = V_f + \frac{kT_e}{2e} \ln\left(\frac{2m_i}{\pi m_e}\right) \quad \text{(Eq. 5)}$$

Since some of the probe techniques provided unrealistically high estimates of electron temperature, many of the calculated plasma potentials are quite high. As such, the contour plot color ranges were chosen to the focus on the area near the cathode orifice, where probe traces tended to be closer to the expected theoretical shapes and analysis was valid. Results can be seen in Figures 12-15.

Single Probe

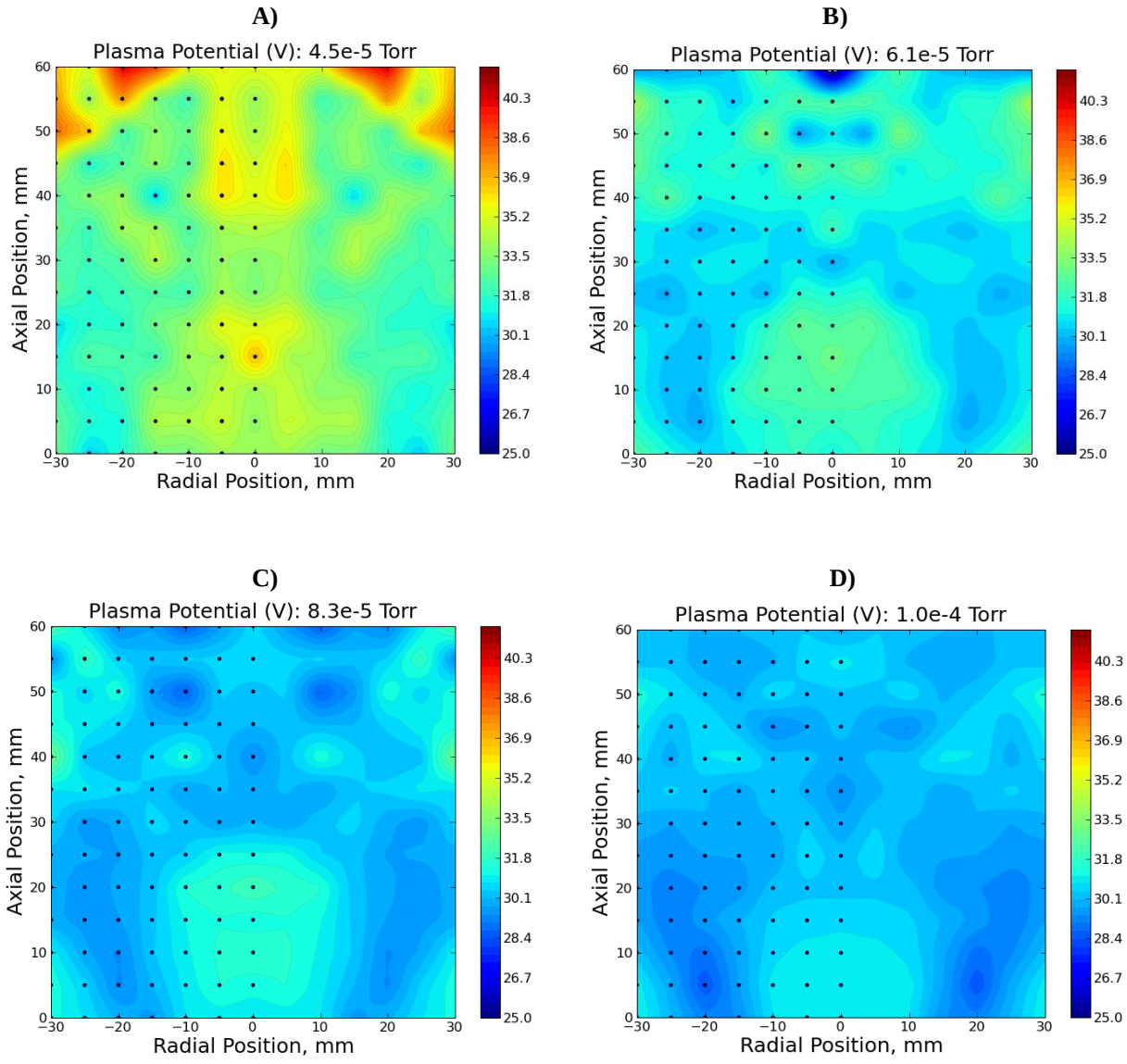

Figure 12. Plasma potential as measured by the single probe at A) 4.5 x 10^{-5} Torr, B) 6.1x 10^{-5} Torr, C) 8.3 x 10^{-5} Torr, and D) 1.0 x 10^{-4} Torr.

Double Probe (Hyperbolic Tangent)

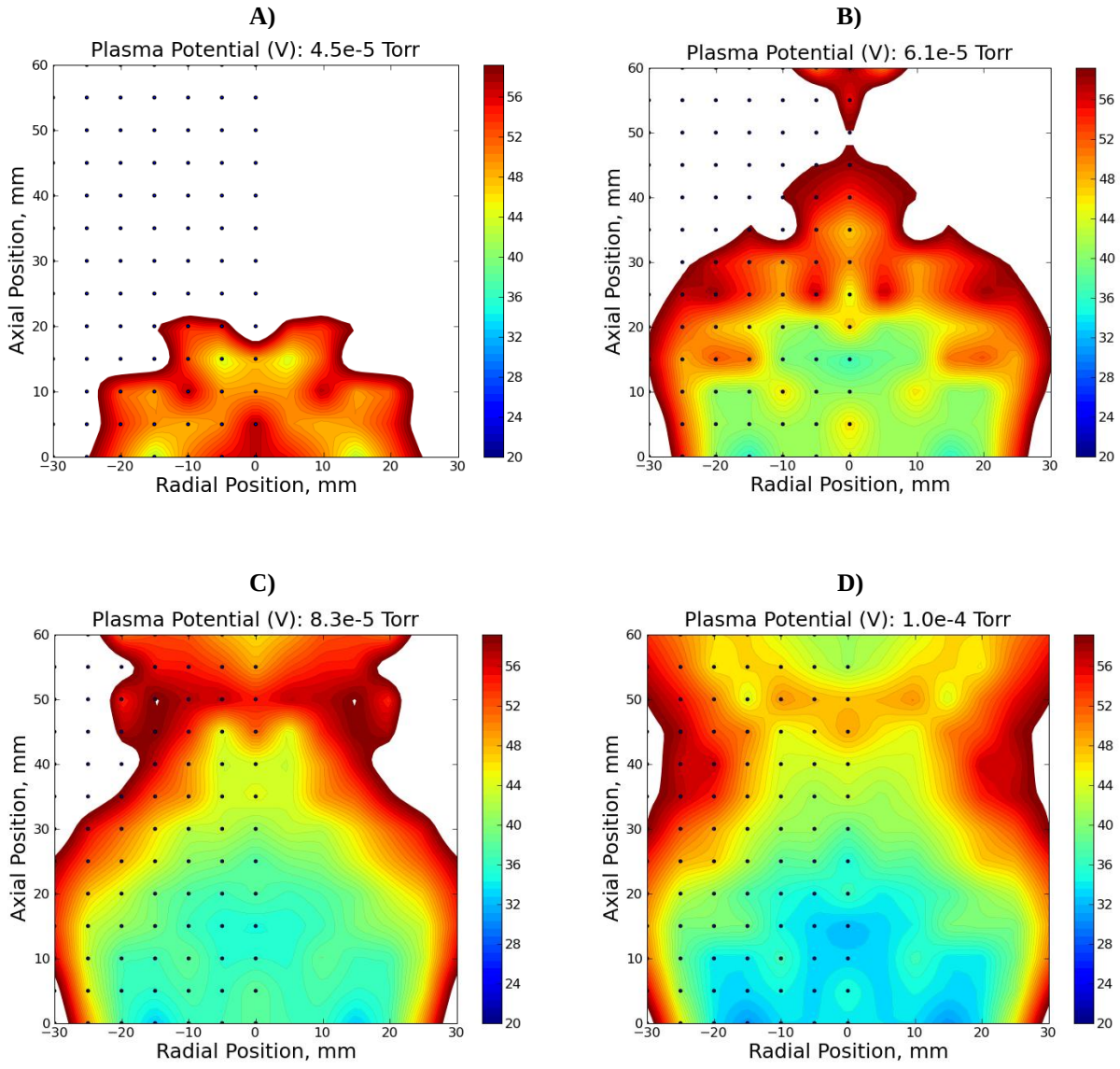

Figure 13. Plasma potential as measured by hyperbolic tangent fit at A) 4.5 x 10^{-5} Torr, B) 6.1x 10^{-5} Torr, C) 8.3 x 10^{-5} Torr, and D) 1.0 x 10^{-4} Torr.

Double Probe (Amemiya)

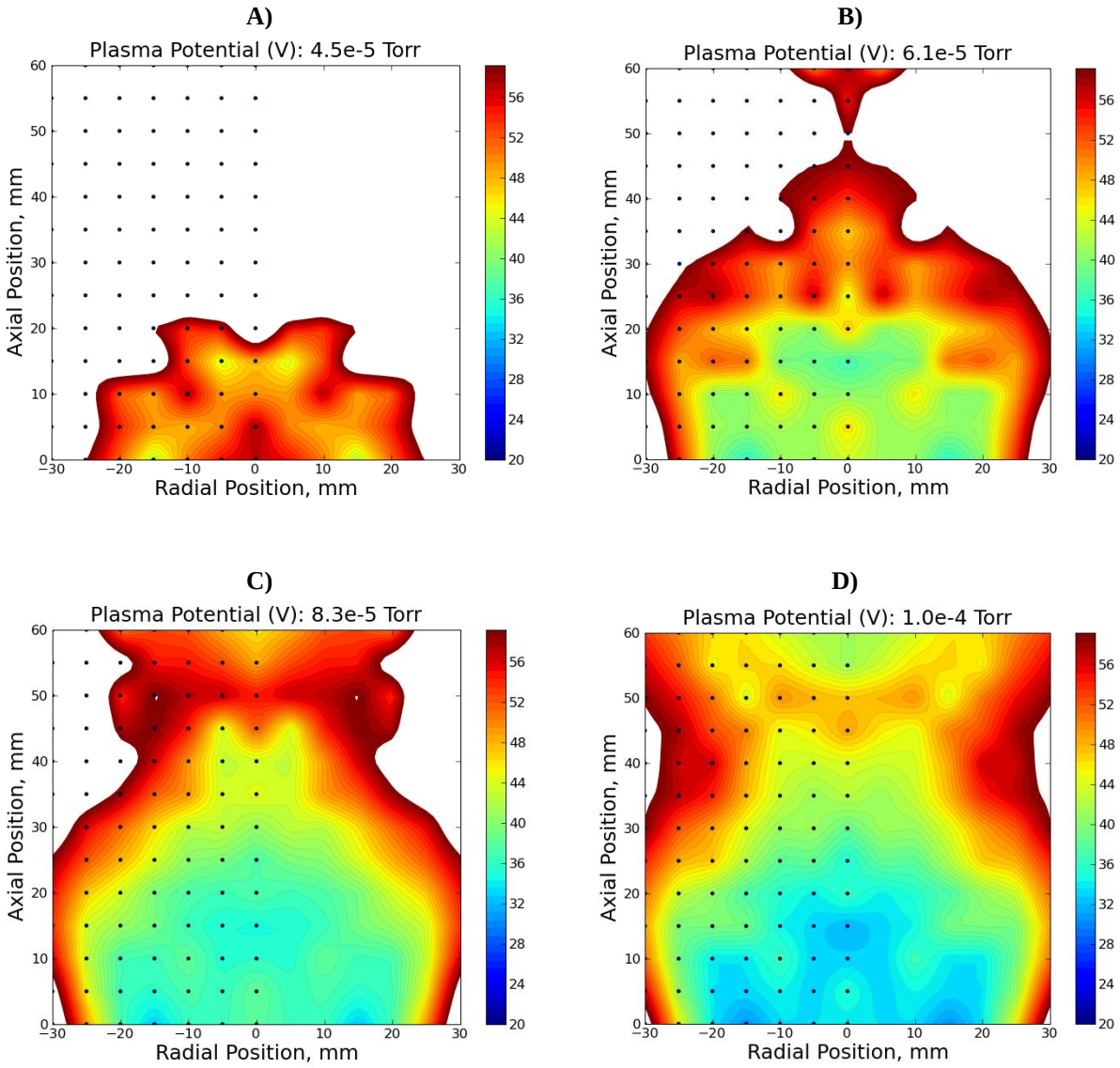

Figure 14. Plasma potential as measured by Amemiya's method at A) 4.5 x 10^{-5} Torr, B) 6.1x 10^{-5} Torr, C) 8.3 x 10^{-5} Torr, and D) 1.0 x 10^{-4} Torr.

Double Probe (Chen)

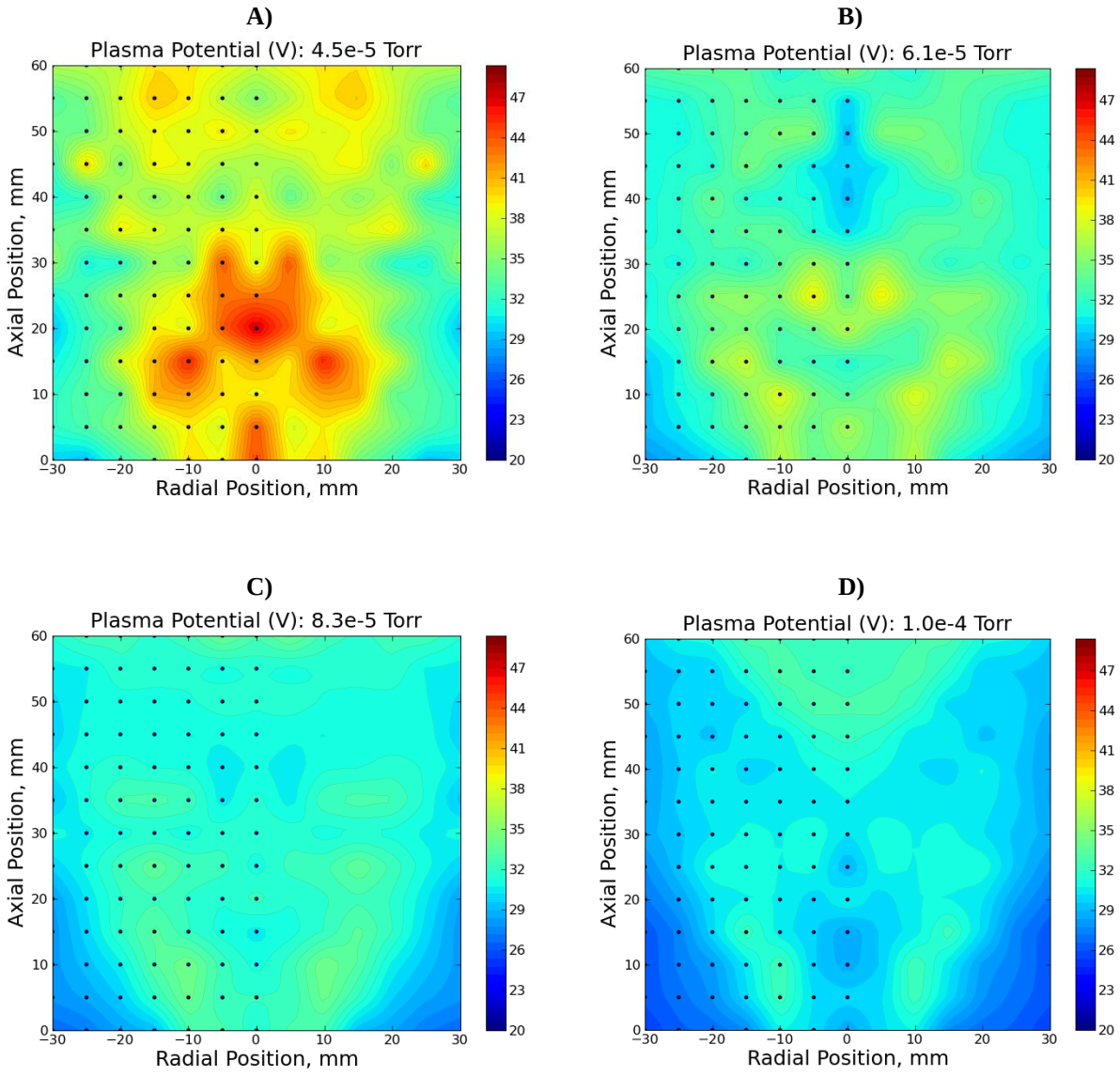

Figure 15. Plasma potential as measured by Chen's method at A) 4.5 x 10^{-5} Torr, B) 6.1x 10^{-5} Torr, C) 8.3 x 10^{-5} Torr, and D) 1.0 x 10^{-4} Torr.

IV. Discussion

A. Electron Density

Calculated density was similar for all four techniques, with the exception that near the orifice the single probe predicted much lower densities than all three of the double probe methods at all pressures. This phenomenon can be seen in Figure 16. As the background pressure was increased, the density near the cathode orifice increased, with a

50% increase in density at the highest background pressure compared to the lowest pressure. At a radius of 20 mm or more from the orifice the density remained essentially unchanged.

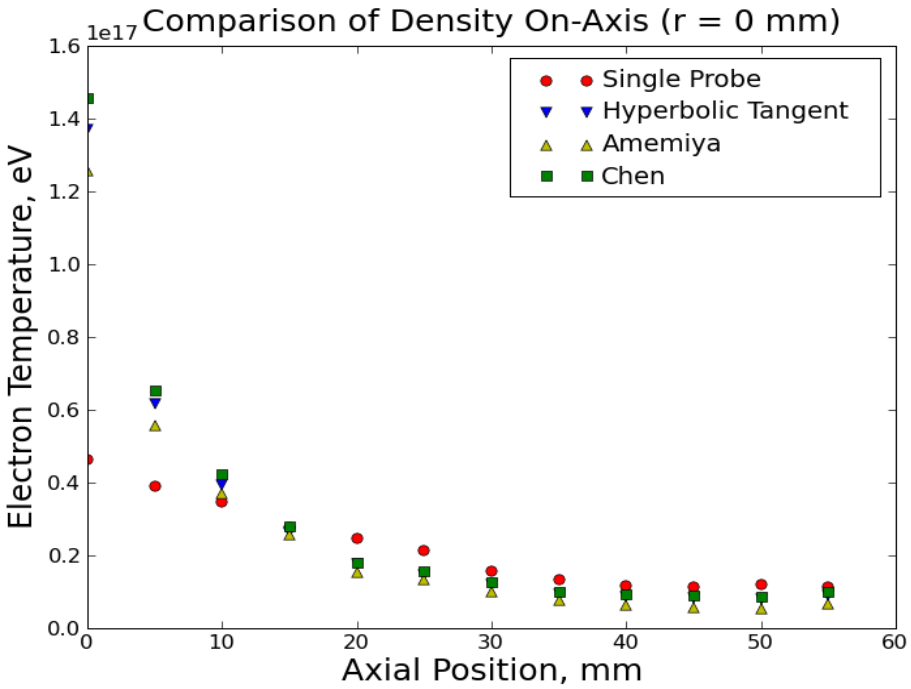

Figure 16. Axial variation of plasma density at 6.1 x 10^{-5} Torr.

B. Electron Temperature

Electron temperature varied by as much as a factor of four over the different methods. Far from the orifice the single probe traces deviated from the expected shape, with no clear knee indicating saturation. Inspection of the single probe ln(I) vs. V curves reveals that the exponential electron current region is not quite linear, indicating that the electron distribution is not fully Maxwellian. As such, the region to perform the linear fit was chosen somewhat arbitrarily. These characteristics can be seen in Figure 17. Compare this to Figure 3, which exhibits a distinct knee. The electron temperatures near the orifice estimated by the single probe are also higher than what others have reported with single probes on LaB_6 cathodes[6], although the cathode operating conditions, anode shape and positioning were different. Given the small electron-neutral collision cross section and low densities found in the cathode plume, the electron mean free path is hundreds of times the anode-cathode separation distance. This indicates the plasma was essentially collisionless, so some electrons may have been accelerated in a beam-like fashion towards the anode. This would lead to higher-energy electrons closer to the anode, and may be responsible for skewed estimates of both electron temperature and plasma potential in regions further than about 3 cm from the cathode orifice.

The hyperbolic tangent method estimates an electron temperature less than that of the single probe, with increasing values when further than 3 cm away from the cathode in many cases. This overestimate is attributed to the poor fit of a hyperbolic tangent to the data. The hyperbolic tangent fit is valid for a Maxwellian plasma, and it appears that the plasma was not fully Maxwellian. The curve was visibly a poor fit near 0 V, which is the region where the temperature is determined. An example of poor fit can be seen in Figure 18. In general, the further from the orifice the poorer the fit, deteriorating faster radially than axially. For comparison, a good fit can be seen in Figure 19.

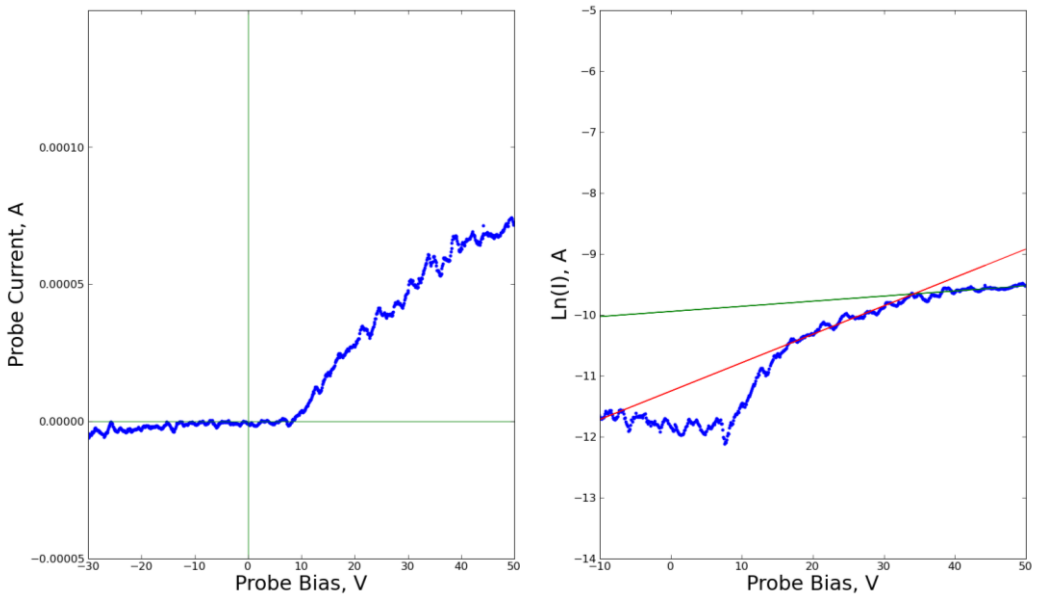

Figure 17. Single probe trace exhibiting poor saturation.

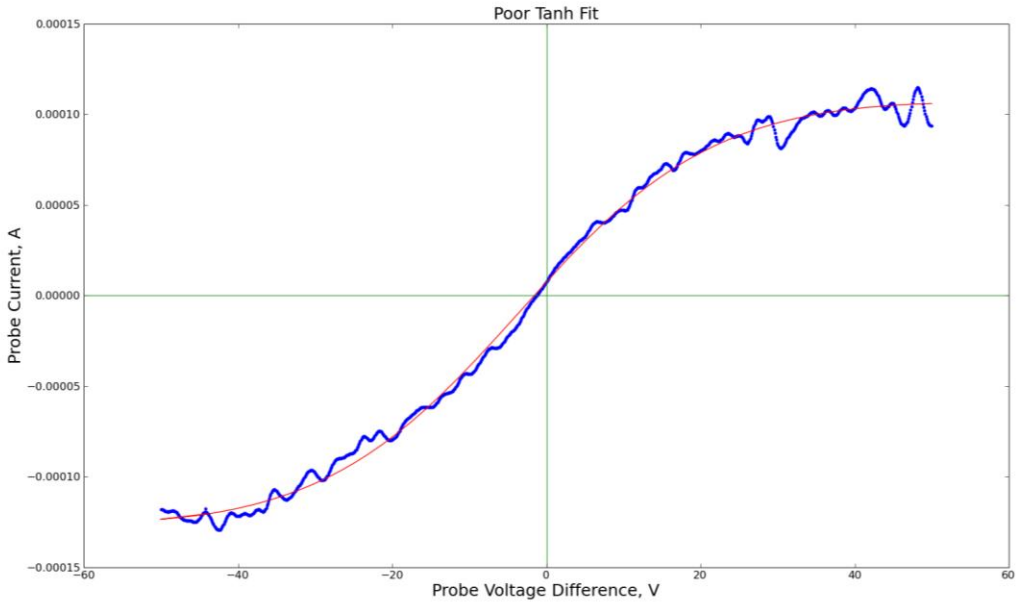

Figure 18. Example of a poor hyperbolic tangent fit, especially near 0 V.

It is difficult to comment on the validity of the method used by Amemiya for two reasons. First, the data were too noisy for direct numerical differentiation, so the differentiation was performed on the sometimes poorly-fit hyperbolic tangent curve. Second, the derivation of the equation that yields the estimate of electron temperature assumes that the I-V characteristic is a hyperbolic tangent in the first place. The conclusion was that applying the Amemiya analysis was of no advantage in this plasma.

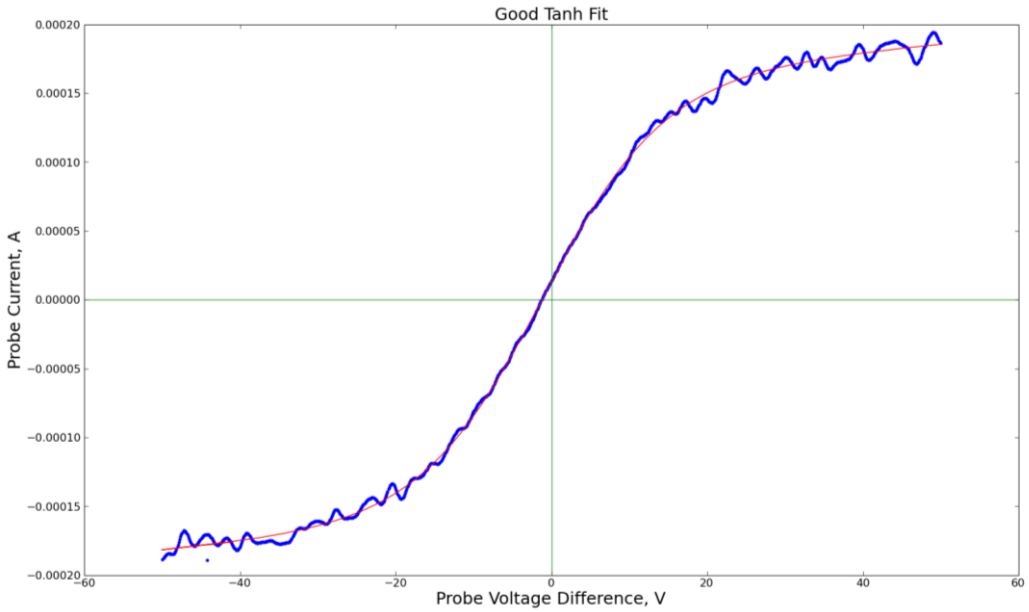

Figure 19. Example of a good hyperbolic tangent curve fit.

Applying Chen's piece-wise linear analysis yielded electron temperatures in the range of 2 to 6 eV and a flat potential structure near the orifice, which is similar to what was found by Fossum and Sommerville[6]. Chen's method also did not generate the anomalous values that the other methods did, since deviation from an ideal hyperbolic tangent I-V characteristic affected it the least. As traces deteriorated with increasing distance from the cathode, the central region from which electron temperature is determined was affected the least. Chen's method is also the simplest to implement. A representative comparison of on-axis temperature can be seen in Figure 20.

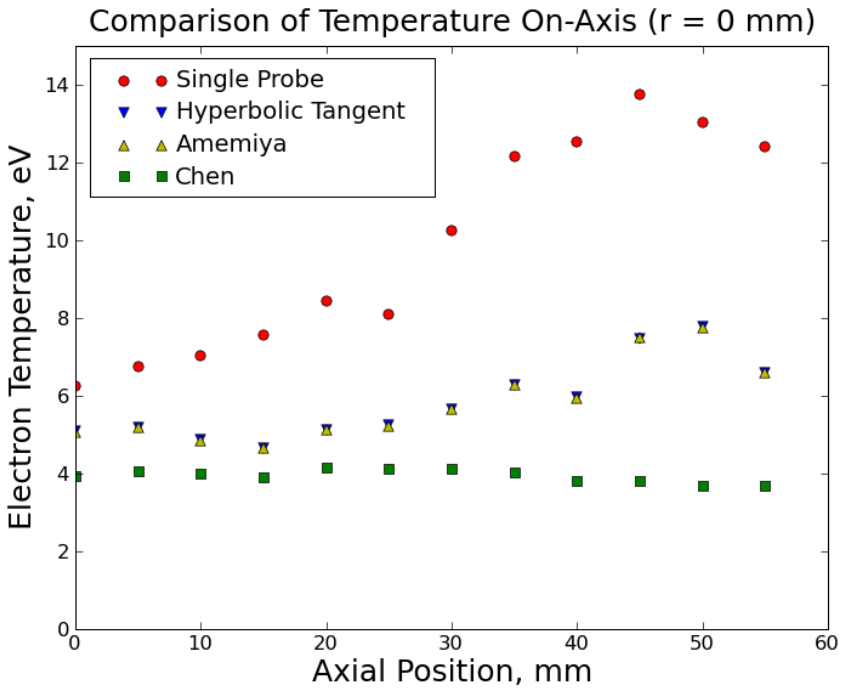

Figure 20. Temperature comparison, 8.3 x 10^{-5} Torr.

C. Plasma Potential

The single probe yielded a relatively flat potential structure, with plasma potential in the range of 28 to 40 V. The hyperbolic tangent and Amemiya calculations yield much higher plasma potentials on the fringes of the data map, due to the large estimates of electron temperature they produce when far from the orifice, and are not considered valid in those regions. Closer to the orifice the plasma potential is more in line with that measured by the single probe.

The plasma potential structure predicted by the Chen method is different that the others, with a distinct island of increased plasma potential two centimeters downstream of the orifice with no argon backfill. With argon flowing into the chamber the plasma potential ranges from 25 to 35 V. This flatter potential near the orifice may explain the lower electron energies indicated by this method.

V. Conclusions

Several probe analysis techniques were compared in an attempt to establish baseline data to be compared against a laser Thomson Scattering system in the future. The hyperbolic tangent fit and the Amemiya method both generated significant anomalies when more than 30 mm from the cathode and were determined to be unreliable in the cathode plasma used in this work. This is attributed to the non-Maxwellian nature of the plasma, and possibly low plasma density as the probes are moved away from the cathode. Low density leads to excessive variation in the saturation regions, and the noise makes the Amemiya method extremely difficult to employ. The single probe method depends on an exponential electron current (a Maxwellian distribution), and this also was not found. The fit had to be applied more arbitrarily than the authors wanted, and as such the data is not regarded as particularly accurate. The most reliable method was Chen's technique for double probe analysis, which yielded reasonable measurements and was the simplest to employ, as no arbitrary fits had to be made.

Acknowledgments

The first author would like to thank Mark Hopkins for constructing the cathode used in this work, and for spending a great deal of his time helping troubleshoot hardware. The first author would also like to thank Jerry Ross for his immense help in automating the data acquisition portion of this project. This work was supported by the U.S. Air Force Office of Scientific Research.

References

[1] Mott-Smith, H. M., and Langmuir, I., "The Theory of Collectors in Gaseous Discharges", *Physical Review*, Vol. 28, 1926, pp. 727-763.

[2] Huddlestone, R. H., and Leonard, S. L., *Plasma Diagnostic Techniques*, Academic Press, Inc., New York, 1965, Chap. 4.

[3] Muraoka, K., Uchino, K., and Bowden, M., **"**Diagnostics of low-density glow discharge plasmas using Thomson scattering", *Plasma Phys. Control. Fusion*, Vol. 40, 1998, pp. 1221-1239.

[4] Pace, D., "Example of Langmuir Probe Analysis", 2007, University of California, Irvine, http://www.davidpace.com/physics/graduate-school/langmuir-analysis.htm

[5] Amemiya, H., "Plasmas with negative ions – probe measurements and charge equilibrium", *J. Phys. D: Appl. Phys.*, Vol. 23, 1990, pp. 999-1014.

[6] Fossum, E. C., Sommerville, J. D., and King, L. B., "Characterization of Near Field Plasma Environment of a Hollow Cathode Assembly", AIAA-2004-3795, *40th AIAA/ASME/SAE/ASEE Joint Propulsion Conference*, July 12-14, Fort Lauderdale, Fla.